KSTLE International Journal, Vol. 2, No. 2, December 2001, pp. 114-119

Theoretical Analysis of Magnetic Flux Density Distribution in an Electro-Magnetic Chuck

Chung Kyun Kim†

Department of Mechanical and Design Engineering, Hongik University

Abstract : The distribution of magnetic flux density of electro-magnetic chucks may clarify the clamping characteristics, which is strongly related to the machining efficiency and machining accuracy in surface grinding machine. Therefore the distribution of the normal and the tangential components of magnetic flux density have been analyzed theoretically. It appears that the normal component of magnetic flux density increases and the tangential component of magnetic flux density increases as the ratio of the separator width to the pitch, *e/p* decreases. The results seem to increase the stability and uniformity of normal component of magnetic flux density for the decreased *e/p*.

Key words : Magnetic flux density, friction coefficient, chuck, machining accuracy, Biot-Savart law

Introduction

The electro-magnetic chuck is one of the most convenient fixtures of the workpiece and normally associated with grinding operations. And the electro-magnetic chuck has been widely used to reduce set-up times on the grinding machine, planers and milling machines, because of its easiness of operation and possibilities to get high parallelism without difficulties. Hall and Chadwick [1] have found that the electro-magnetic chuck is one of effective tools on other metal cutting machines. In general, the electro-magnetic chuck may reduce set-up times by around 65% compared with other convenient working units on milling machine and planers.

With an increasing demand of machine tools, the machining accuracy, reliability and productivity have been more important for the analysis of machine-tool-workholding unit as a whole. Unfortunately, there are few research works relating to the performance of interfaces between the workholding unit and the workpiece in the electro-magnetic chuck. Although the electro-magnetic chuck is widely used as a fixture, no fundamental research has been made due to its complex characteristics. Nakano [2] presented that the clamping condition is related to the chattering, machining efficiency, and machining limit. The chucking force of rectangular electro-magnetic chucks using the gauss meter and the load cell was measured by Saito *et al.* [3].

There are many factors affecting the chucking force of electro-magnetic chucks, which are the chucking position, current, magnetic flux density, surface contact conditions, contact area, pitch length, and width of separator. In this study, we are especially interested in the distribution of magnetic flux density. This may clarify the clamping characteristics, which is strongly related to the machining efficiency and machining accuracy.

In this paper, the distribution of magnetic flux density has been analyzed for a rectangular electro-magnetic chuck theoretically. This may make clear the chucking characteristics of electro-magnetic chucks, which are closely related to the machining efficiency and machining accuracy of machine tools.

Theoretical Analysis

In order to analyze the chucking characteristics of electro-magnetic chucks, the distribution of magnetic flux density over the chucking surface has to be known. This can be accomplished by applying Biot-Savart law to the chuck.

Fig. 1 shows the geometry for a rectangular coil carrying a current. x and y axes are fixed in perpendicular and parallel to

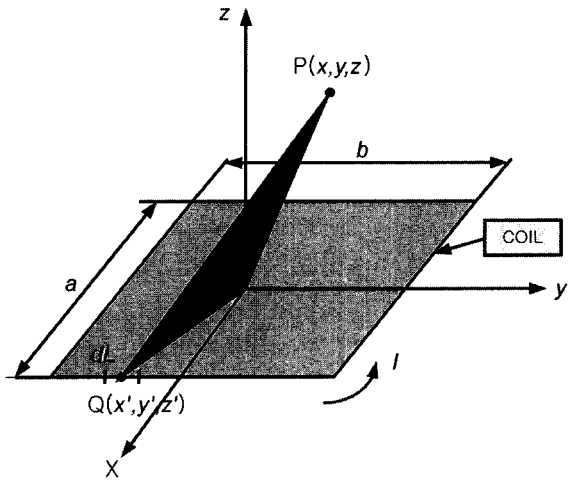

Fig. 1. Magnetic field intensity in a closed rectangular path.

†Corresponding author; Tel: 82-2-320-1623, Fax: 82-2-323-8793
E-mail: ckkim@wow.hongik.ac.kr

the direction of the separator, respectively. z axis is vertical to the face plate surface. $\boldsymbol{I}_x$, $\boldsymbol{I}_y$ and $\boldsymbol{I}_z$ are unit vectors directed along the positive x, y and z axes, respectively. In this model, the magnetic field intensity, bold $\boldsymbol{H}$ for a line current distribution is obtained by integrating the contributions from all the incremental elements:

$$\boldsymbol{H} = \frac{\mu_0}{4\pi}\int_L \frac{I d\boldsymbol{L} \times \boldsymbol{I}_{QP}}{\boldsymbol{R}^2} \tag{1}$$

where μ_0 is the permeability of free space, $\boldsymbol{I}$ is a current, $d\boldsymbol{L}$ is a differential length of wire, $\boldsymbol{R}$ is a distance from any point Q on each side of the top to the arbitrary point P where the magnetic field intensity is to be found. A boldface letter denotes a vector quantity.

In order to determine the total magnetic field intensity, we apply Biot-Savart law equation (1) to the rectangular coil element as shown in Fig. 1. The total magnetic field, $\boldsymbol{H}_t$ about this path is then given by the sum of the four values as:

$$\boldsymbol{H}_t(x, y, z) = \boldsymbol{H}_f + \boldsymbol{H}_b + \boldsymbol{H}_l + \boldsymbol{H}_r \tag{2}$$

where $\boldsymbol{H}_f$ is the magnetic field of left coil given by

$$\boldsymbol{H}_f = \int_{-b/2}^{b/2} d\boldsymbol{H}_f = \frac{\mu_0 I}{4\pi}\left[-z\boldsymbol{I}_x + \left(x - \frac{a}{2}\right)\boldsymbol{I}_z\right] \frac{y - y'}{[(x - a/2)^2 + z^2][(x - a/2)^2 + (y - y')^2 + z^2]^{1/2}} \Bigg|_{y' = -b/2}^{y' = b/2}$$

$\boldsymbol{H}_b$ is the magnetic field of back coil given by

$$\boldsymbol{H}_b = \int_{-b/2}^{b/2} d\boldsymbol{H}_b = \frac{\mu_0 I}{4\pi}\left[z\boldsymbol{I}_x - \left(x + \frac{a}{2}\right)\boldsymbol{I}_z\right] \frac{y - y'}{[(x + a/2)^2 + z^2][(x + a/2)^2 + (y - y')^2 + z^2]^{1/2}} \Bigg|_{y' = -b/2}^{y' = b/2}$$

$\boldsymbol{H}_l$ is the magnetic field of left coil given by

$$\boldsymbol{H}_l = \int_{-a/2}^{a/2} d\boldsymbol{H}_l = \frac{\mu_0 I}{4\pi}\left[z\boldsymbol{I}_y - \left(y + \frac{b}{2}\right)\boldsymbol{I}_z\right] \frac{x - x'}{[(y + b/2)^2 + z^2][(x - x')^2 + (y + b/2)^2 + z^2]^{1/2}} \Bigg|_{x' = -a/2}^{x' = a/2}$$

$\boldsymbol{H}_r$ is the magnetic field of right coil given by

$$\boldsymbol{H}_r = \int_{-a/2}^{a/2} d\boldsymbol{H}_r = -\frac{\mu_0 I}{4\pi}\left[z\boldsymbol{I}_y - \left(y - \frac{b}{2}\right)\boldsymbol{I}_z\right] \frac{x - x'}{[(y - b/2)^2 + z^2][(x - x')^2 + (y - b/2)^2 + z^2]^{1/2}} \Bigg|_{x' = -a/2}^{x' = a/2}$$

For any magnetic material in which the magnetization, $\boldsymbol{M}$ is proportional to the magnetic flux, $\boldsymbol{H}$ the magnetic flux density, $\boldsymbol{B}$ is given by

$$\boldsymbol{B} = \mu_0(1 + \chi_m)\boldsymbol{H} \quad \mu_0\mu_r\boldsymbol{H} \tag{3}$$

where χ_m is a magnetic susceptibility and μ_r $(=1 + \chi_m)$ is a relative permeability. This equation may be used for any homogeneous, linear, isotropic magnetic material that may be described in terms of a relative permeability.

It is assumed that the edge effects of $\boldsymbol{B}$ does not exist in the y direction. Then the absolute magnitude of magnetic flux density on the chuck surface, i.e., $z = 0$ is uniform along the x direction as shown in Fig. 2. The magnetic flux density leaving through N pole is the same to that of entering through S pole. Based upon these assumptions, this can be modeled for $z = 0$ as shown in Fig. 3. The fluctuating magnetic flux density with the exponentially decreasing properties of magnetic flux in the z direction may then be expressed by

$$f(x, z) = \begin{cases} -|B_0| e^{-n\pi z/(p+e)} & \text{for } -(p+e) < x < -e \quad \text{and} \quad z \geq 0 \\ 0 & \text{for } -e < x < 0 \quad \text{and} \quad z \geq 0 \\ |B_0| e^{-n\pi z/(p+e)} & \text{for } 0 < x < p \quad \text{and} \quad z \geq 0 \\ 0 & \text{for } p < x < p + e \quad \text{and} \quad z \geq 0 \end{cases} \tag{4}$$

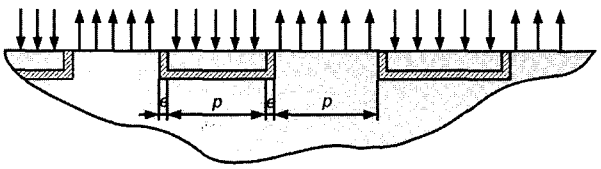

Fig. 2. A periodic magnetic flux density is uniformly distributed along the x direction when z is zero.

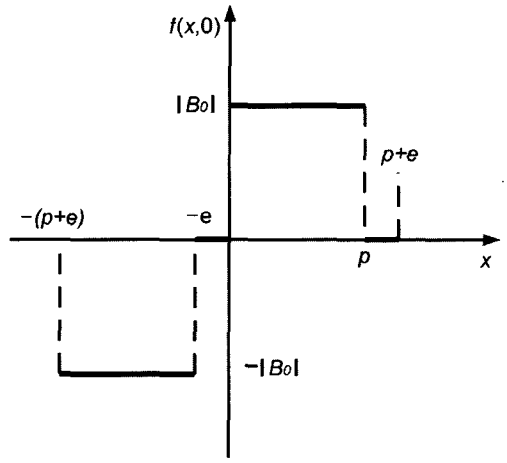

Fig. 3. Uniform magnetic flux on the face plate surface when z is zero.

where $|B_0|$ is the magnetic flux density which is emitted from the face plate surface of the magnetic chuck to the free space. p is a pitch of the pole and e is a width of separator as shown in Fig. 2.

Using a Fourier series, the periodic magnetic flux density can be written as a function of x and z components. Therefore,

$$f(x,z) = \frac{|B_0|}{\pi}\sum_{n=1}^{\infty}\frac{1}{n}\left[a_n\cos\frac{n\pi x}{(p+e)} + b_n\sin\frac{n\pi x}{(p+e)}\right]e^{-\frac{n\pi z}{(p+e)}} \tag{5}$$

where

$$a_n = \sin\frac{n\pi p}{(p+e)} + \sin\frac{n\pi e}{(p+e)}$$

$$b_n = -\cos\frac{n\pi p}{(p+e)} + \cos\frac{n\pi e}{(p+e)} - \cos n\pi + 1$$

The normal and tangential components of magnetic flux density can be derived from Eq. (5). Then,

$$\Gamma_n = \frac{|B_0|}{(p+e)}\sum_{n=1}^{\infty}\left[a_n\cos\frac{n\pi x}{(p+e)} + b_n\sin\frac{n\pi x}{(p+e)}\right]e^{-\frac{n\pi z}{(p+e)}} \tag{6}$$

$$\Gamma_t = \frac{|B_0|}{(p+e)}\sum_{n=1}^{\infty}\left[a_n\sin\frac{n\pi x}{(p+e)} - b_n\cos\frac{n\pi x}{(p+e)}\right]e^{-\frac{n\pi z}{(p+e)}} \tag{7}$$

The ratio, Γ_t/Γ_n of the tangential flux density to the normal flux density is given by

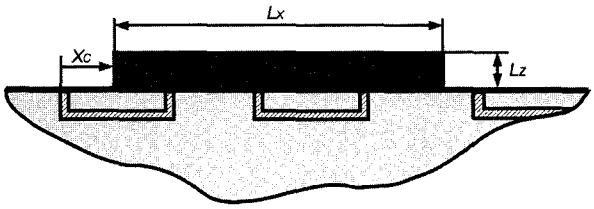

Fig. 4. Chucking position of workpiece.

$$\frac{\Gamma_t}{\Gamma_n} = \sum_{n=1}^{\infty}\frac{\left[a_n\sin\frac{n\pi x}{(p+e)} - b_n\cos\frac{n\pi x}{(p+e)}\right]e^{-\frac{n\pi z}{(p+e)}}}{\left[a_n\cos\frac{n\pi x}{(p+e)} + b_n\sin\frac{n\pi x}{(p+e)}\right]e^{-\frac{n\pi z}{(p+e)}}} \tag{8}$$

The normal component of chucking force, F_n is given in reference [4] as:

$$F_n = \int_0^{L_z}\int_{Xc}^{L_x+L_c}\frac{\Gamma_n^2}{2\mu}dxdz \tag{9}$$

The normal chucking force was numerically calculated when the workpiece is placed on the chuck surface as shown in Fig. 4. Here L_x and L_z are the dimensions of the workpiece in the x and z directions, respectively. x_c denotes an arbitrary position from the separator.

The tangential component of chucking force will continuously try to move the workpiece on the chuck surface until it is balanced with the frictional force. The tangential component of chucking force, F_t may then be given by

$$F_t = f(W + F_n) \tag{10}$$

where f is a coefficient of friction between the workpiece and the face plate of the chuck, W is a weight of workpiece. This equation explains that the coefficient of friction may be an important factor on the analysis of chucking characteristics. When the weight of workpiece is small compared with the normal chucking force, the tangential component of chucking force is directly proportional to the normal chucking force.

$$F_t \fallingdotseq fF_n \tag{11}$$

Results and Discussion

In Figs. 5(a)~5(e), the dimensionless normal components of magnetic flux density are plotted as a function of the horizontal chucking position x for various values of the vertical chucking position z. In these figures, the absolute value of normal flux density decreases as the vertical distance over the plate surface of the chuck increases. It is shown that the flux density is strong near the edge of the separator as the vertical chucking position z approaches to the plate surface. To investigate the effect of the separator, the ratio of the width of the separator to the pitch length was varied from $e/p = 0$ to 2.67. In Figs. 5(a)~5(e), as the width of the separator increases, the dimensionless normal component of magnetic flux density decreases near the separator and particularly concentrates its intensity on the

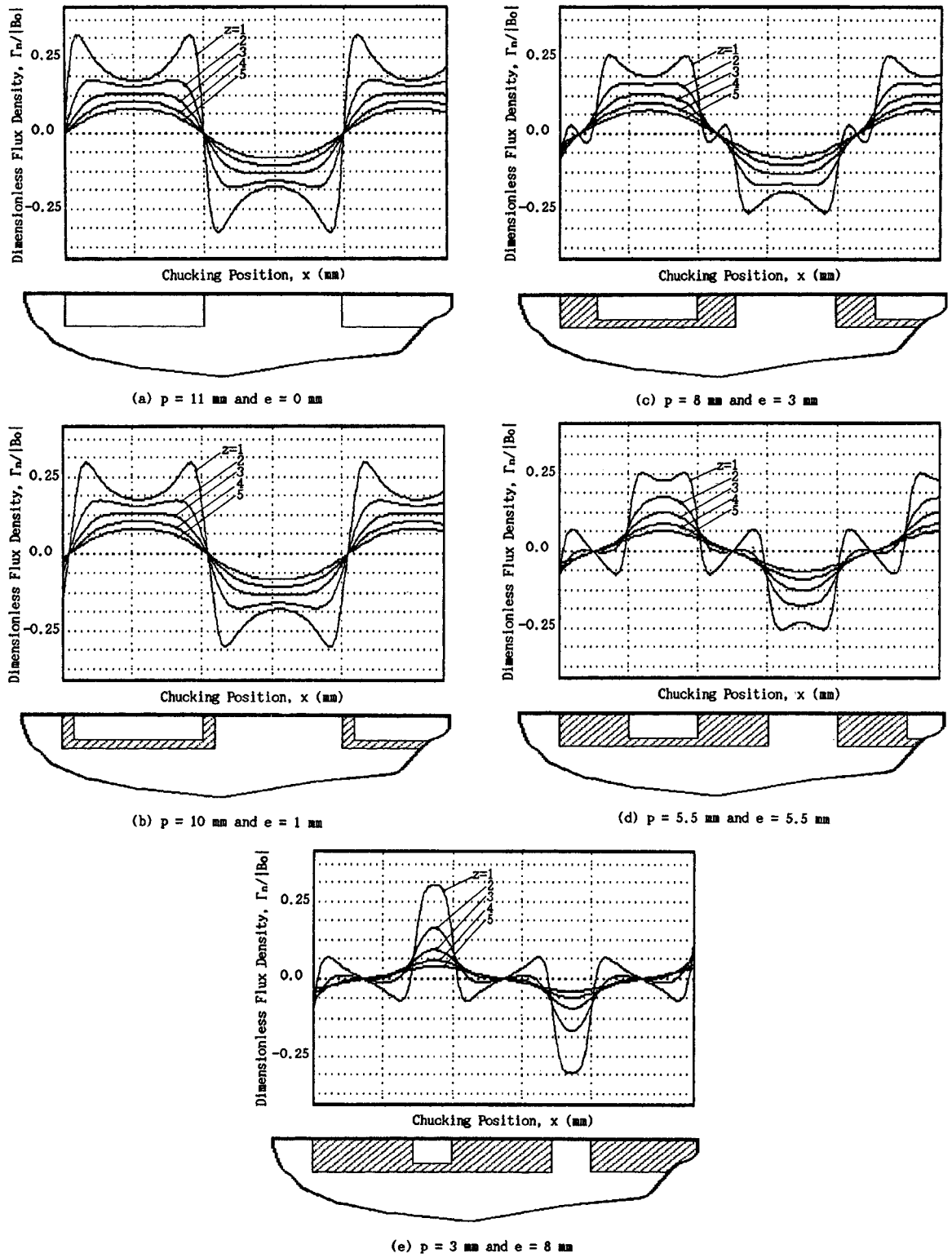

Fig. 5. Effect of vertical chucking position z and horizontal position x on dimensionless normal component of magnetic flux density.

center of the pitch length p for the higher value of e/p. This may explain that the increased width of the separator is not desirable for the chucking system and may produce the unstable chucking force due to the distorted distribution of normal component of magnetic flux density. This will affect the machining accuracy of the workpiece.

In Figs. 6(a)~6(e), the dimensionless tangential components of magnetic flux density are plotted as a function of the horizontal chucking position x for various values of the vertical chucking position z over the chuck surface. In these figures, the

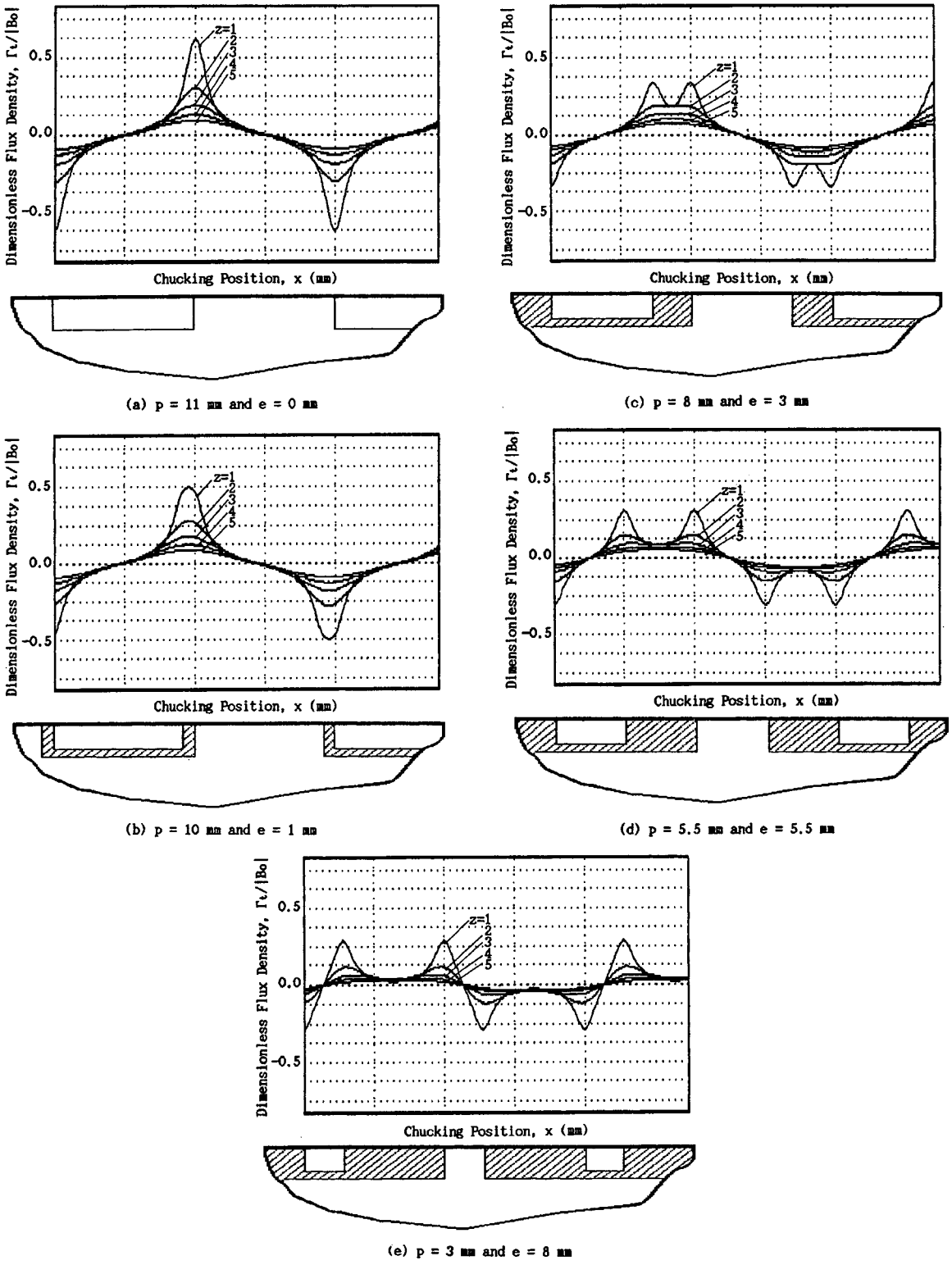

Fig. 6. Effect of vertical chucking position z and horizontal position x on dimensionless tangential component of magnetic flux density.

absolute value of tangential flux density decreases as the vertical distance z over the plate surface increases. The ratio of the width of the separator to the pitch length was changed from $e/p = 0$ to 2.67 as shown in Figs. 6(a)~6(e). These figures show that as the width of the separator increases, the dimensionless tangential component of magnetic flux density decreases and shows two peaks separated from the single peak. The tangential component of the magnetic flux density is strongly related to the friction force, which is very important of the chucking force. The center of the magnetic chuck is located on

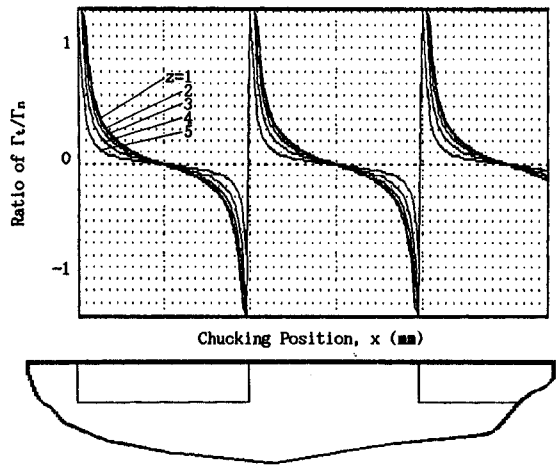

Fig. 7. Ratio of the tangential flux density to the normal flux density for p=11 mm and e=0 mm.

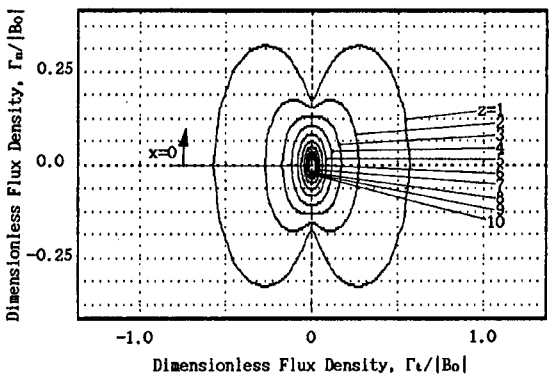

Fig. 8. Distribution of magnetic flux density for p=11 mm and e=0 mm.

the left and right edges of the separator. In particular, the magnitude of tangential components of magnetic flux density is increasingly decreased for $z \rightarrow 0$ as the width of the separator increases. Figs. 5(a) and 6(a) show the similar curves which are demonstrated by Saito *et al.* [3] for the small value of *e/p*.

Fig. 7 shows the ratio of the tangential flux density to the normal flux density for various values of the vertical chucking position z over the plate surface. As the horizontal chucking position on the plate surface increases, the ratio of the tangential flux density to the normal flux density decreases in hyperbolic shape. This means that the effect of the tangential component of flux density diminishes rapidly as the chucking position x approaches to the center of the pitch length.

In Figs. 8(a) and 8(b), the tangential and normal components of flux density replotted for various values of the vertical chucking position z. As z approaches to the face plate surface, the curve of the tangential flux density to the normal flux density shows the peanut shape for $p = 11$ mm and $e = 0$ mm shown in Fig. 8(a) and the distorted peanut figure for $p =$ 10 mm and $e = 1$ mm as shown in Fig. 8(b). In these figures, the tangential flux density is zero at the center of the pitch and the normal flux density is zero at the center of the separator. As we can expect from the figures 5(a)~5(e) and 6(c)~6(e), which are plotted for the increased ratio of $e/p = 0.38$, 1 and 2.67, the symmetric shape of the peanut will especially be distorted for z 0. As the vertical chucking position over the face plate surface increases, the magnetic flux density decreases rapidly and the figure is changed from the peanut shape to the elliptical one.

Conclusion

The distribution of magnetic flux density has been analyzed for electro-magnetic chucks. As the ratio of the separator width to the pitch, *e/p* decreases, the normal component of magnetic flux density increases. This may lead to increase the chucking force of the chucks. The decreased ratio of *e/p* increases the tangential component of magnetic flux density and produces the concentration of the flux density of the center of the separator. Therefore, it will be very important to consider the ratio of the separator width to the pitch of the pole piece, *e/p* as a design parameter. The optimal ratio of *e/p* should be selected for the balanced chucking force between the normal and tangential components of magnetic flux density. The machining accuracy of machine tools may be influenced by the ratio of *e/p*. In general, the normal and tangential components of magnetic flux density increase strongly as the vertical chucking position over the plate surface approaches to the face surface of the chuck. The computed results appear to increase the stability and uniformity of normal component of magnetic flux density for the decreased *e/p*. For any values of *e/p*, the tangential magnetic flux density is zero at the center of the pitch and the normal flux density zero at the center of the separator.

References

1. Hall and Chadwick, Electro-Magnetic Chucks Widen Appeal, Machinery and Production Engineering, Vol. 139, No. 3375, pp. 2324, August 1981.
2. Nakano, Y., The Effect of Methods for Chucking Workpieces and Tools on Machining Accuracy, J. of JSPE, Vol. 44, No. 11, pp. 1299-1307, 1978.
3. Saito, Y. Nishiwaki, N. Ootani, T. and Okimoto, K., Study on the Chucking Force of an Electro-Magnetic Chuck, Bulletin of JSME, Vol. 28, No. 237, pp. 515-522, 1985.
4. Hayt, W. H., Engineering Electromagnetics, 4th ed., McGraw-Hill, 1981.